Journal of Dispersion Science and Technology

ISSN: (Print) (Online) Journal homepage: https://www.tandfonline.com/loi/ldis20

Chicken feathers derived materials for the removal of chromium from aqueous solutions: kinetics, isotherms, thermodynamics and regeneration studies

Rupa Chakraborty , Anupama Asthana , Ajaya Kumar Singh , Renu Verma , Sreevidya Sankarasubramanian , Sushma Yadav , Sónia A. C. Carabineiro & Md. Abu Bin Hasan Susan

To cite this article: Rupa Chakraborty , Anupama Asthana , Ajaya Kumar Singh , Renu Verma , Sreevidya Sankarasubramanian , Sushma Yadav , Sónia A. C. Carabineiro & Md. Abu Bin Hasan Susan (2020): Chicken feathers derived materials for the removal of chromium from aqueous solutions: kinetics, isotherms, thermodynamics and regeneration studies, Journal of Dispersion Science and Technology, DOI: 10.1080/01932691.2020.1842760

To link to this article: https://doi.org/10.1080/01932691.2020.1842760

JOURNAL OF DISPERSION SCIENCE AND TECHNOLOGY
https://doi.org/10.1080/01932691.2020.1842760

Chicken feathers derived materials for the removal of chromium from aqueous solutions: kinetics, isotherms, thermodynamics and regeneration studies

Rupa Chakraborty[a], Anupama Asthana[a], Ajaya Kumar Singh[a], Renu Verma[a], Sreevidya Sankarasubramanian[a,b], Sushma Yadav[a], Sónia A. C. Carabineiro[c], and Md. Abu Bin Hasan Susan[d]

[a]Department of Chemistry, Govt. V. Y. T. PG. Autonomous College, Durg, Chhattisgarh, India; [b]Department of Chemistry, Kalyan PG College, Bhilai Nagar, Durg, Chhattisgarh, India; [c]LAQV-REQUIMTE, Department of Chemistry, NOVA School of Science and Technology, Universidade NOVA de Lisboa, Caparica, Portugal; [d]Department of Chemistry, University of Dhaka, Dhaka, Bangladesh

ABSTRACT

In the present study, chicken feathers (CFs), obtained from animal waste, were used as bio-adsorbent for the removal of hazardous Cr(VI) ions from aqueous solutions. Fourier transform infrared spectroscopy (FTIR), scanning electron microscopy (SEM), energy-dispersive x-ray spectroscopy (EDX), x-ray diffraction (XRD), adsorption of N_2 at −196 °C, thermogravimetric analysis (TGA), and point of zero charge (pH_{pzc}) determination were used to characterize the adsorbent. The N_2 adsorption results revealed high surface area and microporous structure for the adsorbent. The experimental results in batch adsorption show that optimum conditions are: pH 2.5, equilibrium contact time 180 minutes, concentration of CFs 11 g L^{-1}, and initial Cr(VI) concentration 25 mg L^{-1}. The experimental data on Cr(VI) adsorption were fitted using the Langmuir and Freundlich equations at different temperatures. The Langmuir adsorption model showed the best fit. The maximum monolayer capacity (q_{max}) of CFs was found to be 333.33 mg/g. The kinetic results of Cr(VI) ion were fitted to four kinetic models: pseudo-first-order, pseudo-second-order, intra-particle diffusion, and Elovich . The pseudo-second-order chemisorption model had a higher coefficient. The thermodynamics data showed that the adsorption process of Cr(VI) on CFs was endothermic and spontaneous. The desorption efficiency and reusability of CFs were determined for three adsorption–desorption cycles, which proved to be very effective for the removal of Cr(VI) ions from aqueous solutions.

ARTICLE HISTORY
Received 10 March 2020
Accepted 12 October 2020

KEYWORDS
Chromium(VI); chicken feathers; adsorption isotherm; kinetics; thermodynamics

GRAPHICAL ABSTRACT

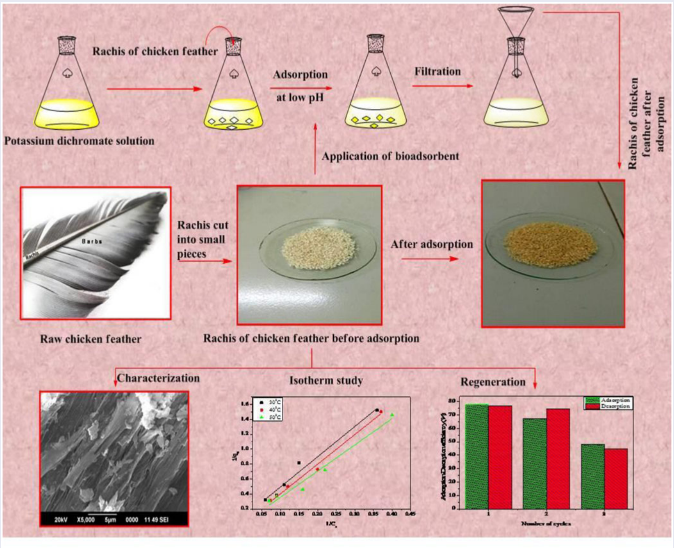

Abbreviations: CFs: chicken feathers; FTIR: Fourier transform infrared ; SEM: scanning electron microscopy; EDX: energy-dispersive x-ray spectroscopy; XRD: x-ray diffraction; BET: Brunauer–Emmett–Teller; TGA: thermogravimetric analysis; DTG: differential thermogravimetry; pH_{pzc}: point of zero charge

CONTACT Ajaya Kumar Singh ajayaksingh_au@yahoo.co.in Department of Chemistry, Govt. V. Y. T. PG. Autonomous College, Durg-491001, Chhattisgarh, India.

Supplemental data for this article is available online at https://doi.org/10.1080/01932691.2020.1842760.

1. Introduction

The rapid industrialization in the last few decades has been a major cause for environmental pollution. Several organic and inorganic pollutants are present in the atmosphere. Heavy metal ions are one of the most toxic and carcinogenic contaminants. Moreover, they are non-biodegradable and present in air, water, and soil.[1,2] Various heavy metal ions are released into water streams, which affect the quality of water supply. Some are poisonous and accumulate in the tissues of living organisms.

Chromium is noxious due to its non-biodegradable nature and it is present in the list of top 20 contaminants and hazardous materials in the last 15 years.[3,4] It can be found in the environment mainly in the Cr(III) and Cr(VI) valence states. Toxicity of trivalent chromium is negligible, but the hexavalent form of chromium is 500 times more toxic and carcinogenic than trivalent chromium.[5] The increased use of chromium in industrial applications, such as electroplating, metallurgy, tanning, textile dyeing, and preservation of food, poses serious threats to ecosystems. Cr(VI) exists in different anionic forms such as hydro chromate ($HCrO_4^-$), chromate (CrO_4^{2-}), or dichromate ($Cr_2O_7^{2-}$) anions, which depend on the pH of aqueous solution. Cr(VI) ions are structurally similar to oxyanions, viz. phosphates and sulfates and they can actively enter inside the cell.[6] It causes cancer in the digestive tract, headache, diarrhea, nausea, vomiting, lung tumor, and hemorrhage. When Cr(VI) ions enter inside the cell, they form stable bonds with protein and DNA. This can show several mutagenic effects such as genotoxicity and mutagenicity.[6] The Environmental Protection Agency (EPA) set the allowed limit of chromium in drinking water as 0.1 mg/L.[7]

Various methods are reported for the removal of Cr(VI) from wastewater, including chemical precipitation,[8] ion exchange,[9] membrane separation,[10] and reverse osmosis.[11] However, these procedures involve high cost and have low feasibility, which hinder their wider application. Adsorption is one of the preferred methods for Cr(VI) removal, since they show their high efficiency and low cost.[12] Activated carbon is very effective for the adsorption of Cr(VI), but their use is limited due to the inherent costs of fabrication. Therefore, better alternatives are needed. For heavy metal removal, bio-adsorption method provides a natural, eco-friendly, and low-cost alternative method.[13]

In recent years, eyes have been pointed on natural materials derived from wastes from agricultural and industrial activities as potential inexpensive alternatives for Cr(VI) removal. In general, adsorbents derived from agricultural by-products or waste materials coming from other industries are considered as “low-cost adsorbents”.[14,15] Many examples of natural adsorbents for wastewater treatment have been reported to remove Cr(VI), including mangosteen peel,[16] sugarcane bagasse,[17] sawdust,[18] litchi peel,[19] apricot shell,[20] and honeydew peels.[21]

Chicken feathers (CFs) are an interesting and abundant animal waste material. Several million pounds of waste feathers are obtained and discarded by the poultry processing plants. CFs contain around 90% of keratin proteins, which can form α-helix (41%), β-sheet (38%), and disordered structures (21%).[22,23] Keratin is a biopolymer, which contains hydroxyl, carboxyl, and amine groups that act as binders of the metal ions so as to remove them from wastewater.[24–26] In previous studies, barb parts of CFs were used for the removal of toxic dyes.[27–30] Several researchers also reported that barb parts of CFs can also be used for adsorption of heavy metal ions present in aqueous solutions.[31–33] There have been no reports on the use of rachis of CFs. Furthermore, studies so far reported only minor characterizations using Fourier transform infrared (FTIR) spectroscopy and scanning electron microscopy (SEM) and detailed characterizations of the adsorbent are yet to be reported. Thus, despite various studies on biomass characterization and application, further investigation of CFs with detailed characterization of CFs still remains an elusive goal.

In the present study, we used the rachis part of CFs and found out that this bio-adsorbent is very effective, low cost, and does not require any modification in the reactions. Rachis of CFs is expected to have relatively high specific surface area and good thermal stability than other low-cost adsorbents. In our previous research work, we have used barb parts of CFs modified with sodium hydroxide and ethylene diamine and the specific surface area was found to be 16 m^2/g, which removed heavy metal ions.[34] Therefore, in our present work, we have used rachis part of CFs to exploit their high specific surface area as compared to barb parts of CFs to remove Cr(VI) ions in higher amount successfully.

The purpose of this work was to test CFs for the adsorption of chromium from aqueous solutions. FTIR, SEM, energy-dispersive x-ray spectroscopy (EDX), x-ray diffraction (XRD), adsorption of N_2 at $-196\,^\circ C$, thermogravimetric analysis (TGA), and point of zero charge (pH_{pzc}) were used to characterize the material. The influence of different parameters was investigated, which include: contact time, pH, amount of adsorbent dosage, and initial Cr(VI) concentration. The data of Cr(VI) adsorption were analyzed by means of adsorption isotherms and kinetics models.

2. Experimental

2.1. Preparation of Cr(VI) solution and determination of analytical concentration

A stock solution of Cr(VI)(1000 ppm) was prepared by dissolution of a required amount of potassium dichromate ($K_2Cr_2O_7$) in double-distilled water. Standard solutions with the desired concentration were obtained by dilution of the original stock solution. Concentrations of chromium were obtained before and after the tests and analyzed by UV-Vis spectrophotometry using the diphenylcarbazide method, as described in the literature.[34,35] A pink-purple colored complex formed by the reaction of Cr(VI) and 1,5-diphenylcarbazide in acidic medium formed a complex of pink-purple color, whose absorption was measured at 540 nm. Adjustment of pH was made using 0.1 M HCl and 0.1 M NaOH solutions. All the chemicals were of analytical grade and purchased from Hi-Media and Merck Laboratories Pvt. Ltd. (India).

2.2. Preparation of adsorbent and its characterization

Raw CFs were collected from a poultry processing plant of Durg, Chhattisgarh (India). At first, CFs were washed with detergent and tap water and then rinsed with distilled water

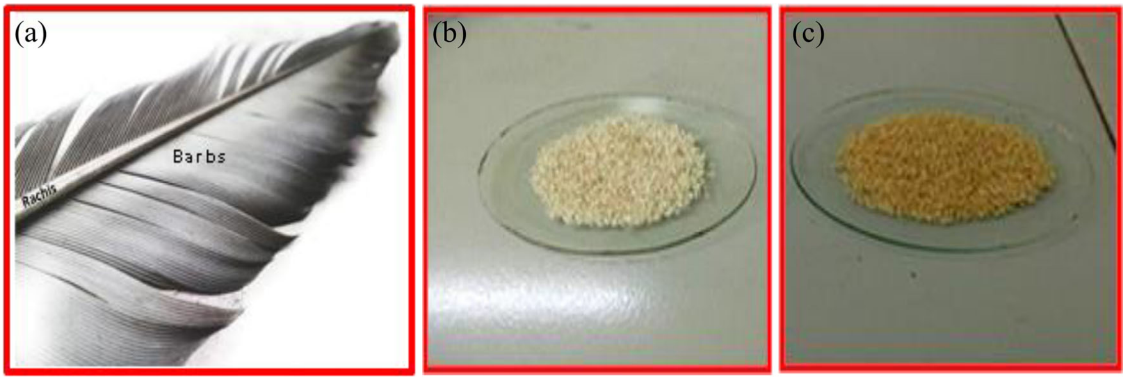

Figure 1. (a) Image of CFs; rachis of CFs (b) before and (c) after adsorption of Cr(VI).

several times. CFs were dipped into aqueous ethanol (20% v/v) for 12 hours, to completely remove organic residues and again rinsed with double distilled water. The washed CFs were dried, the barbs were removed and the rachises were cut into small pieces with scissors. The rachis is the central shaft of the feather (Figure 1a). The adsorbent was then stored in a desiccator for further use.

The characterization of the adsorbent is very important to understand the adsorption process. The functional groups present in CFs were determined by FTIR spectroscopy (using a Thermo Nicolet, Avatar 370) and the spectra were recorded from 400 to 4000 cm^{-1}, using 32 scans and 4 cm^{-1} of resolution. The dried samples were pulverized in mortar and pestle to obtain fine powder and mixed with 100 mg KBr (spectroscopic grade). The morphology was determined by SEM (JEOL JSM-6390). EDX spectroscopic (EDS, OXFORD XMX N) analysis was used to confirm the adsorption of chromium on the surface of CFs. The XRD pattern was obtained in a XRD equipment (PANalytical-X'Pert3 powder) with Cu-Kα radiation, in the 5–30° at 2θ angles range. N_2 adsorption–desorption analysis was carried out by using a surface area and pore analyzer (BELSORP-mini II, BEL Japan Inc.) at −196 °C. The dry powder samples were pretreated for 3 hours at 90–130 °C under N_2 gas to remove any surface adsorbed water or gas using a pretreatment unit (BELPREP flow II, BEL Japan Inc.). The specific surface areas of CFs were calculated using the Brunauer–Emmett–Teller (BET) method. Pore size distributions were calculated by the Barrett–Joyner–Halenda (BJH) method. Thermogravimetric (TG) measurements (PerkinElmer STA 6000 TG/DT model) were carried out in a N_2 atmosphere flowing at a heating rate of 10 °C min^{-1} using 1.53 mg of the sample from 30 to 565 °C. The pH_{pzc} was determined by taking 5 mL of KNO_3 solutions in different flasks. Initial pH values (pH_i) of KNO_3 solutions were maintained at the pH range of 2–10 using 0.1 M HCl or 0.1 M NaOH. Then 0.1 g of adsorbent was added to each flask. After shaking for 24 hours, the suspension was filtered and the final pH values of the solutions (pH_f) were recorded. The pH_{pzc} was obtained from the plot of ($pH_i - pH_f$) versus pH_i.

2.3. Batch adsorption study

These experiments were carried out in 100 mL borosil flasks, varying different parameters, such as contact time (30–200 minutes), pH (2.0–6.0), adsorbent dose (5–13 g/L), sorbate concentration (5–30 mg/L), and temperature (303–323 K). A water bath incubator shaker (Tempstar) and pH meter (Systronics Digital pH Meter-802) were used. 10 mL of Cr(VI) solution with known concentration and the proper amount rachis of CFs (Figure 1b) were mixed in each flask. 0.1 M HCl and 0.1 M NaOH were used for pH adjustment and then flasks were placed in a water bath incubator shaker. After adsorption, the solutions were immediately filtered to recover the adsorbent (Figure 1c) and the filtrate containing the Cr(VI) solution was analyzed by UV-Vis spectrophotometry (Systronics UV-Vis spectrophotometer-117) using 1,5-diphenylcarbazide at the absorption maximum of 540 nm.

The amount (%) of Cr(VI) removal was calculated by the following equation:

$$R\ (\%) = \frac{C_0 - C_e}{C_e} \times 100 \qquad [1]$$

The amount of Cr(VI) ion adsorbed (q_e) in mg/g was calculated by the following equation:

$$q_e = \frac{C_0 - C_e}{m} \times V \qquad [2]$$

where C_0 and C_e are, respectively, the initial and equilibrium concentrations of Cr(VI) ions (mg/L) in the aqueous solution, m is the adsorbent mass (g), and V is the solution volume (L).

2.4. Desorption and regeneration tests

Desorption, regeneration, and reusability experiments were carried out in a similar way to the adsorption tests. 0.110 g of CFs were used for the adsorption of 25 mg/L (ppm) Cr(VI) ion aqueous solution (10 mL) at pH 2.5, then CFs were filtered and dried in an oven. Then, the metal-loaded CFs were mixed with 0.5 M NaOH (10 mL) and the mixture was shaken at 150 rpm in an orbital shaking incubator. This procedure aimed at determining the CFs reusability and consecutive adsorption–desorption cycles were repeated three times. The eluted adsorbent (CFs) was washed with distilled water several times to remove the desorbing agent. The desorption percentage (%D) was calculated by the equation:

$$\text{Regeneration ratio}\ (\%D) = \frac{C_{des}}{C_0} \times 100 \qquad [3]$$

where C_0 is the initial concentrations of Cr(VI) ions before

Table 1. Physicochemical characterization of CFs.

Parameters	Values
Moisture content (%)	1.00
Ash content (%)	1.27
Carbon (%)	68.48
Oxygen (%)	29.88
Sulfur (%)	1.63
pH_{zpc}	7.36
BET surface area (m^2/g)	39.00
Mean pore diameter (nm)	1.50

adsorption and C_{des} is the concentration of Cr(VI) after desorption in the aqueous solution (both in mg/L).[36]

3. Results and discussion

3.1. Characterization of the adsorbents

The physicochemical properties of the adsorbent greatly influence the rate of the removal of Cr ions from the wastewater. The characterization results of CFs are given in Table 1. Proximate and ultimate analyses were carried out by heating a known weight of the sample and considering the weight loss up to 600 °C. The moisture content at 100 °C was found to be 1% and ash content at 600 °C was 1.27%.

3.1.1. FTIR analysis

FTIR spectra allowed analyzing the chemical structure and functional groups of CFs. The FTIR spectra of CFs before and after Cr(VI) adsorption are shown in Figure 2. The broad absorption band observed at 3398 cm^{-1} is attributed to hydroxyl groups (O-H stretch) on the surface of the adsorbent.[34] It shows a significant shift from 3398 to 3685 cm^{-1} (Figure 2a). This reveals that the Cr(VI) ions are binding with (–OH) groups on the surface of the adsorbent. The peak at 2963 cm^{-1} is ascribed to the C–H stretching vibration. The peak at 1643 cm^{-1} is assigned to C = O stretching vibration of amide I. The amide II band occurs at sharp bands of 1541 cm^{-1} and 1446 cm^{-1}, respectively, due to the N–H bending and C–H stretching vibration. The peak at 1248 cm^{-1} can be attributed to the amide III.[34,37,38] The band at 1075 cm^{-1} may be caused by the C–O symmetric stretching vibration. These results show that CFs are rich in metal ion binding functional groups. The FTIR spectrum of Cr(VI) loaded CFs (Figure 2b) shows shifted peak positions at 3685, 2928, 1678, 1535, 1453, 1236, and 1078 cm^{-1}, due to the adsorption of Cr(VI) (Table 2). The reason for these shifts is that the acidic groups are protonated at pH 2.5; these groups are responsible for the adsorption of Cr(VI) ions on CFs.[39,40]

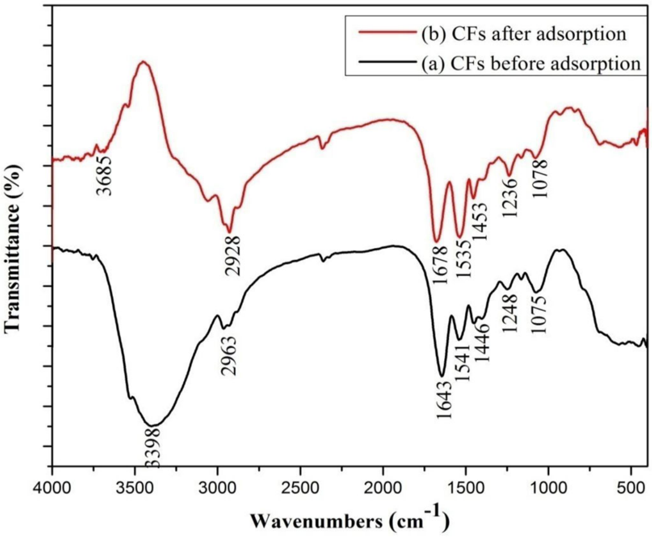

Figure 2. FTIR spectra of CFs (a) before and (b) after chromium adsorption.

Table 2. FTIR spectral characterization of rachis of CFs before and after adsorption.

IR peak	Before adsorption (1/cm)	After adsorption (1/cm)	Assignment
1	3398	3685	–OH stretching
2	2963	2928	C–H stretching
3	1643	1678	C = O stretching (amide I)
4	1541	1535	N–H bending (amide II)
5	1446	1453	C–H stretching (amide II)
6	1248	1236	(Amide III)
7	1075	1078	C–O stretching

3.1.2. SEM analysis

SEM was used to examine the surface morphology of the CFs. SEM images before and after adsorption of chromium are presented in Figure 3a,b, respectively, with 5000× magnification. Figure 3a shows a keratin protein fiber obtained from rachis, which is very thin and hairy. The diameter of the keratin fiber is in the range of 5–50 µm as observed by SEM.[41] The morphology of CFs shows a rough fibrous structure, which is suitable for Cr(VI) adsorption. Figure 3b clearly shows that there are more regularity and smoothness after adsorption of Cr(VI) ions. The formation of a white layer on the surface of the adsorbent shows that Cr(VI) ions are present there.[42]

3.1.3. EDX analysis

EDX analyses were carried out in order to estimate the amount of chromium at the surface of CFs, before and after adsorption, as shown in Figure 3c,d, respectively. Figure 3c shows that CFs possess a maximum of 68.48% carbon on its surface, along with other elements, like oxygen (29.88%) and a minor percentage of sulfur (1.63%), before adsorption of Cr(VI) ions. Since sulfur-containing functional groups of amino acids, such as cysteine, have the ability to chelate heavy metal ions, and because keratin of CFs is very rich in sulfur amino acid groups, the precursor metal ion in solution strongly chelated with the surface. Thus, in Figure 3d, some new chromium peaks were observed due to the adsorption of Cr(VI) on the surface of CFs.

3.1.4. Surface area and pore size analysis

The surface area was determined by the BET method while the BJH method was used for the determination of the average pore size distribution. The obtained data are listed in Table 1. According to the N_2 adsorption–desorption results, the BET surface area of CFs was 39 m^2/g (Supplementary

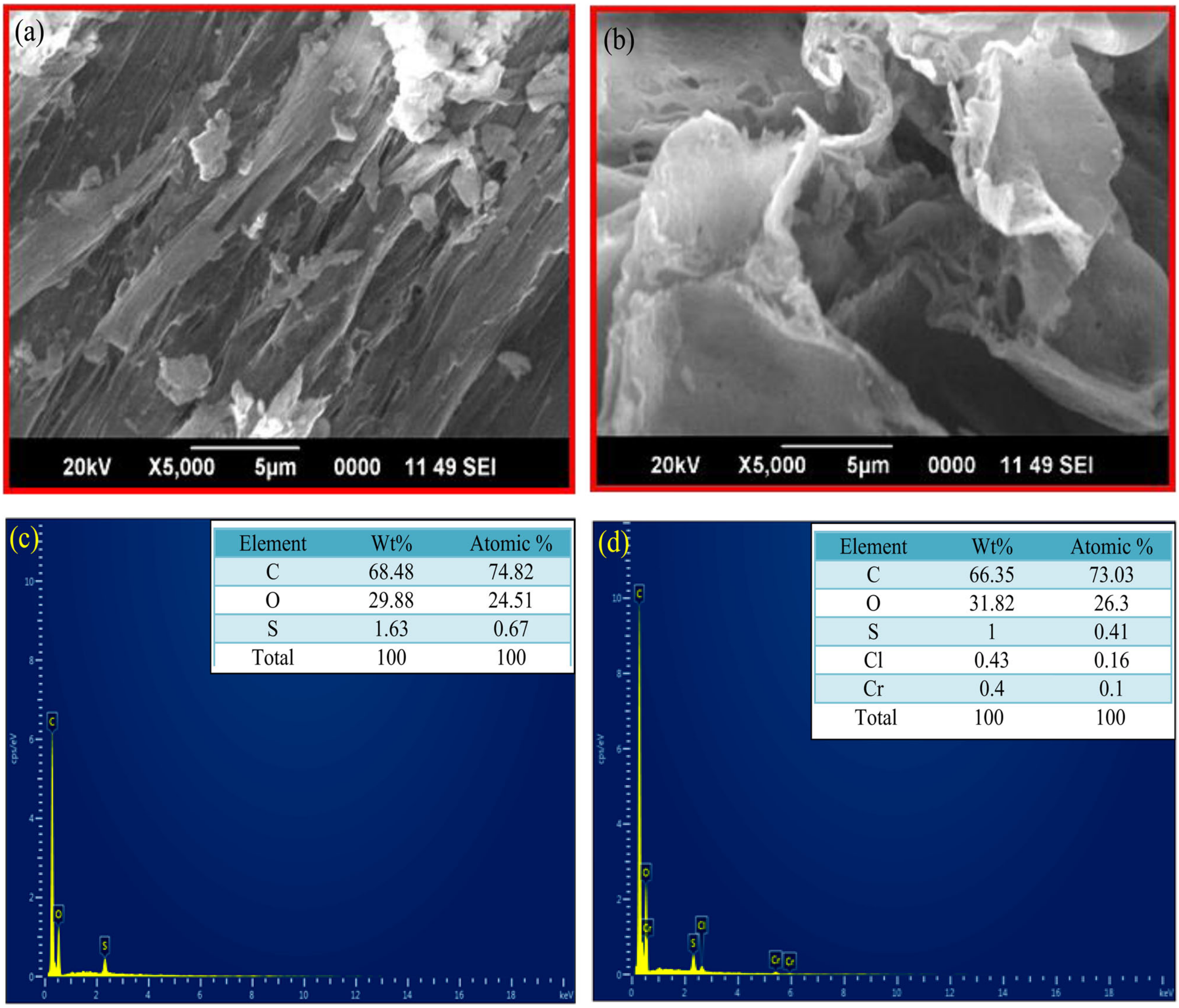

Element	Wt%	Atomic %
C	68.48	74.82
O	29.88	24.51
S	1.63	0.67
Total	100	100

Element	Wt%	Atomic %
C	66.35	73.03
O	31.82	26.3
S	1	0.41
Cl	0.43	0.16
Cr	0.4	0.1
Total	100	100

Figure 3. SEM analysis of keratin fibers from rachis of CFs at 5000× magnification (a) before and (b) after adsorption; EDX analyses of CFs (c) before and (d) after chromium adsorption.

Figure S1) and the BJH pore diameter was 1.5 nm, which is evidence of the microporous nature of this material (Supplementary Figure S2). This shows that the surface area of the CFs is higher than other adsorbents, such as hydrochar of chestnut outer shell and keekar sawdust.[43,44]

3.1.5. XRD analysis

Supplementary Figure S3 shows the diffraction patterns of CFs. Two broad peaks were observed at 2θ around 9.3° and 19.2°, respectively, indicating the presence of semi-crystalline keratin. The diffraction peak at $2\theta \approx 9.3°$ shows the keratin α-helix conformation, while the peak at $2\theta \approx 19.2°$ is indexed for the β-sheet of keratin protein secondary structure.[45]

3.1.6. Thermal stability

The thermal behavior of CFs was studied by TGA and differential thermogravimetry (DTG). TGA and DTG curves of raw CFs are shown in Figure 4a. Three stages of weight loss occurred: from room temperature to around 220 °C, from 220 to 450 °C, and from 450 to 565 °C. In the first stage, weight loss of 8.33% during heating of CFs was up to 220 °C, which corresponds to the loss of surface adsorbed moisture.[46] In the second decomposition zone, from 220 to 450 °C, a significant weight loss was obtained (75.9%), due to the decomposition of the organic matter and the remaining moisture. Finally, the third stage, above 450–565 °C, showed no significant weight loss. DTG of CFs showed two exothermic peaks at 45 and 330 °C.[47] The fastest weight loss rate of 96.6 μg/min occurred at 330 °C.[48]

3.1.7. Point of zero charge

The determination of the pH_{pzc} of the adsorbent is crucial to understand the adsorption mechanism. The cationic adsorption was facilitated at $pH > pH_{pzc}$, while the anionic adsorption was preferred at $pH < pH_{pzc}$.[49] The results of Figure 4b show that the pH_{pzc} of CFs was high (7.36). For a pH_{pzc} value larger than the pH of the solution, the surface of CFs will have a positive charge, which favors the anionic Cr(VI) ion adsorption.

3.2. Effect of pH

The solution pH is also very important for the adsorption process. Cr(VI) can exist in five main stable forms in aqueous solution, namely H_2CrO_4, $HCrO_4^-$, CrO_4^{2-}, $HCr_2O_7^-$, and $Cr_2O_7^{2-}$, depending on the pH of the solution. CrO_4^{2-} anion of Cr(VI) mainly exists above 6.0 pH. $HCrO_4^-$ and $Cr_2O_7^{2-}$ anions are mostly found in the range of pH 2.0–6.0 and H_2CrO_4 is present when $pH < 1.0$.[50] The effect of pH on Cr(VI) adsorption by CFs was examined and the results are shown in Figure 5a. CFs showed 78.64% removal of Cr(VI) at pH 2.5. When solution pH was increased from 2.0 to 6.0, the amount of removed Cr(VI) decreased continuously. The results show that the lower the pH value, the higher the adsorption of Cr(VI).[51,52] The maximum removal percentage of Cr(VI) was found at pH 2.5, due to a large number of H^+ (hydronium) ions present in the acidic medium, and the surface of CFs became positively charged due to the presence of functional groups. The presence of H^+ deactivated the negatively charged OH^- group present on the adsorbent surface. Therefore, the lower the pH value, the higher the removal of Cr(VI), due to the strong electrostatic attraction between oxy-anions of Cr(VI) and positively charged surface of the adsorbent. On the other hand, for higher pH values, the adsorption decreased due to the occurrence of a large number of OH^- ions, which increase the electrostatic repulsive forces between the negatively charged adsorbent surface and the Cr(VI) anions.

3.3. Effect of contact time

The equilibrium time also influences the removal of metal ions from the aqueous solution. Figure 5b shows this effect on the adsorption of Cr(VI) on CFs up to 180 minutes. 10 mL of a 25 mg L^{-1} metal ion solution was placed in a flask containing 0.110 g of adsorbent and shaken at room temperature. Results show that Cr(VI) was quickly adsorbed in the initial stages, then the removal capacity became slower. The amount of Cr(VI) removed slowly increased up to 120 minutes and the equilibrium time was obtained at 180 minutes. A rapid initial removal was observed, due to the large adsorbent surface area, but then the adsorption process slowed down due to electrostatic repulsion between the adsorbent surface and Cr(VI) ions.[53,54] The maximum percentage removal of Cr(VI) ions was 77.84% at 180 minutes.

3.4. Effect of adsorbent dose

The adsorbent amount is also an important factor, as it shows the capacity of the adsorbent for a given initial concentration of Cr(VI) ions. This effect was determined by varying the amount of adsorbent concentration, which ranged from 5 to 13 g/L. The results are shown in Figure 5c. The Cr(VI) removal increases when adsorbent dosage increases, due to the increase of surface area available for adsorption. Cr(VI) ions quickly adsorbed in the initial stage from 5 g/L to 8 g/L, then the removal efficiency became slower. After that, the adsorbent surface and solution of metal ion concentration reached equilibrium and the removal efficiency was constant.[55] An adsorbent concentration of 11 g/L was an optimum value.[56]

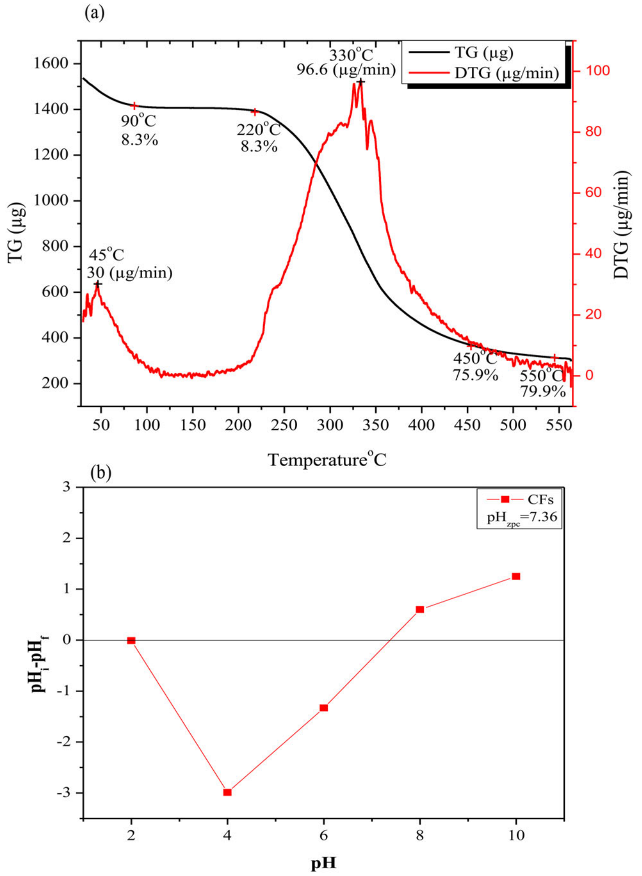

Figure 4. (a) TG–DTG curve of raw CFs; (b) point of zero charge (pHpzc) for CFs.

3.5. Effect of the initial Cr(VI) concentration

The concentration of initial chromium (VI) was varied (5, 10, 15, 20, 25, and 30 mg/L) for experiments at 180 minutes, pH 2.5, 11 g/L adsorbent dose, at room temperature. The results are shown in Figure 5d. The removal efficiency increased with increase in Cr(VI) ion concentration. When the initial Cr(VI) concentration varied from 5 to 30 mg/L, the chromium removal efficiency of the CFs increased from 44% to 77%.[57] In the beginning, the rate of percentage removal of Cr(VI) ions was high due to the large surface area of CFs. Later, as a thick molecular layer was formed over CFs, the adsorption capacity decreased. The initial Cr(VI) concentration determines the equilibrium concentration and removal efficiency of these ions.[58]

3.6. Adsorption isotherms

In order to study the relationship between the adsorbate and adsorbent concentration at equilibrium and the maximum adsorption capacity of adsorbent at a constant temperature, Langmuir and Freundlich isotherm models were used.[59] The isotherm models explained the adsorption process and

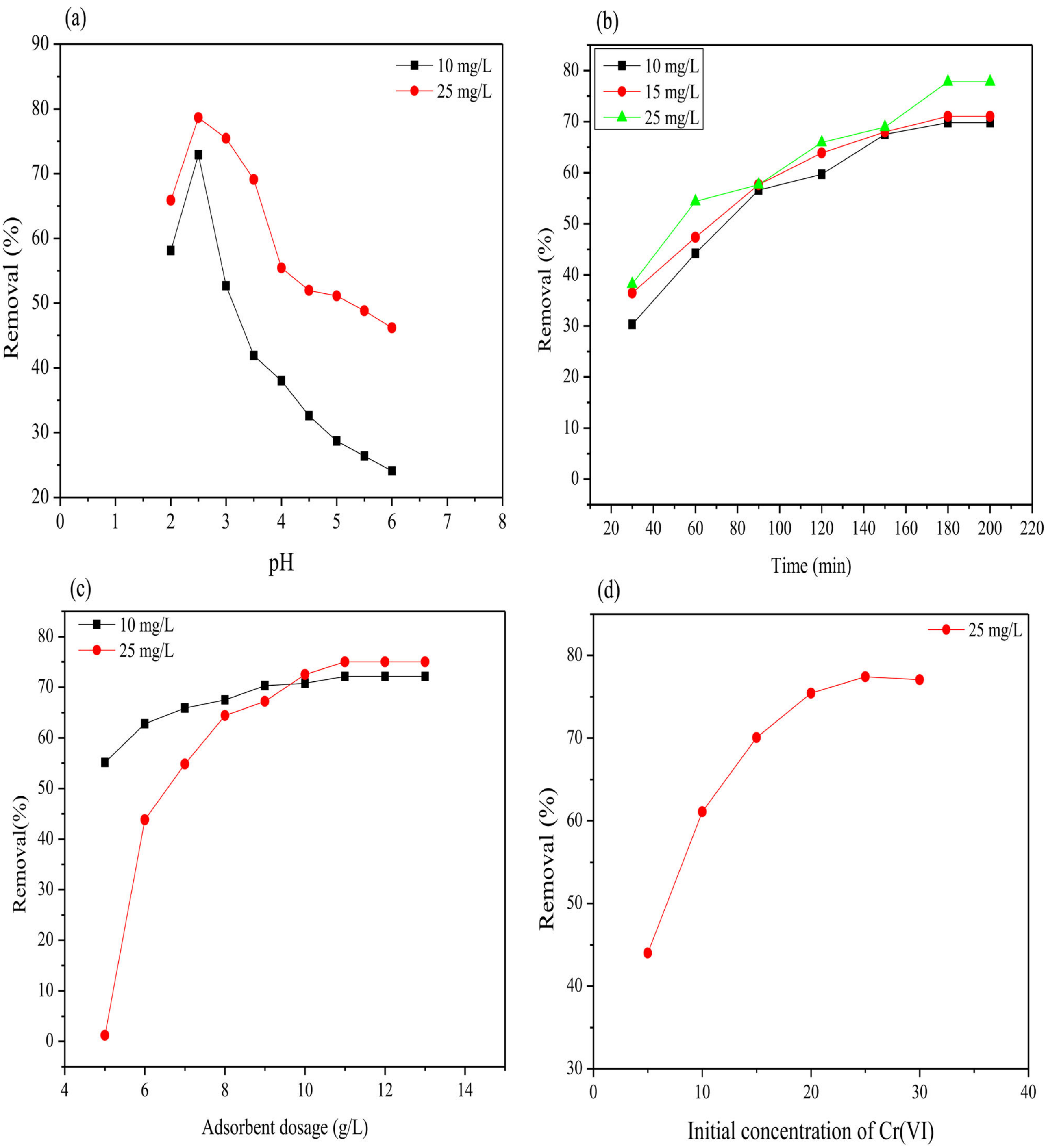

Figure 5. Removal efficiency of Cr(VI) ions using RCFs by batch adsorption study effects of (a) initial pH, (b) adsorption time, (c) adsorbent dosage, and (d) initial concentration of Cr(VI).

gave information on the adsorbent capacity and surface properties. The linear plots of Langmuir and Freundlich isotherm models fitted to the adsorption of Cr(VI) ion on CFs are presented in Figure 6a,b.

3.6.1. Langmuir isotherm model

The Langmuir model assumes that the adsorption of metal ions take a place by monolayer adsorption on a homogenous surface, without any interaction between the adsorbate on adjacent sites.[60] Linear form of Langmuir isotherm model can be represented as:

$$\frac{1}{q_e} = \frac{1}{q_m} + \frac{1}{q_m K_L} \; \frac{1}{C_e} \qquad [4]$$

where q_e is the amount of Cr(VI) adsorbed per amount of adsorbent (mg/g) at equilibrium, q_m is the maximum adsorption capacity, K_L is the Langmuir isotherm constant (L/mg), and C_e is the equilibrium concentration of Cr(VI) in solution (mg/L).

The feasibility of the adsorption process is expressed in terms of a dimensionless separation factor (R_L), which is an essential characteristic of the Langmuir model. The separation factor (R_L) can be calculated by the following equation (5):

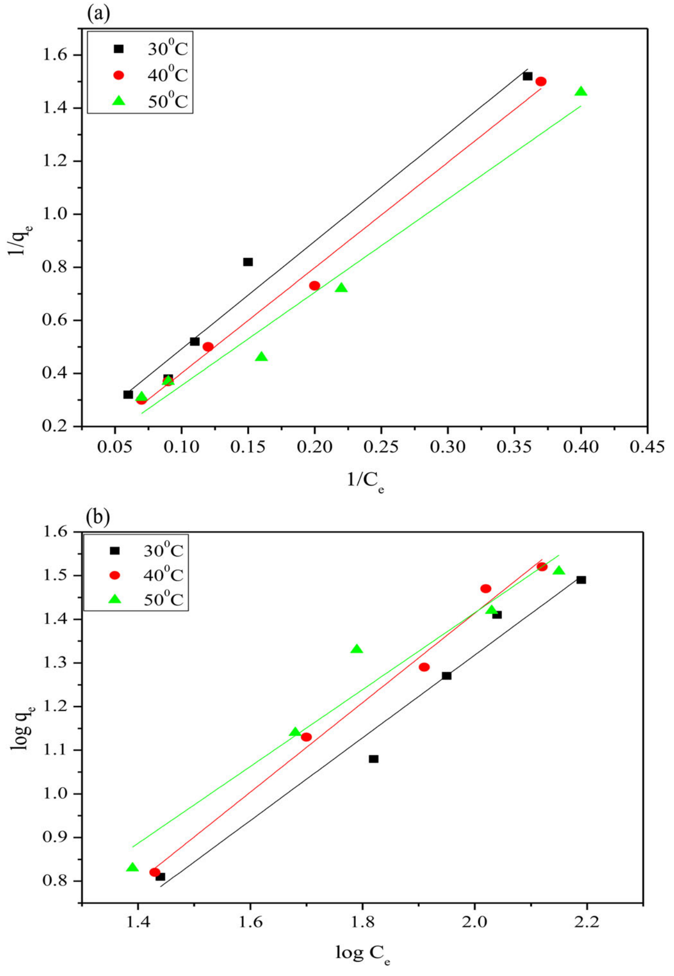

Figure 6. Adsorption isotherms. (a) Langmuir and (b) Freundlich plots for adsorption of Cr(VI) ions onto CFs at different temperatures.

$$R_L = \frac{1}{1 + K_L C_0} \qquad [5]$$

where C_0 is the initial concentration of Cr(VI). The R_L value is an indication that the isotherm and the adsorption process are unfavorable ($R_L > 1$), linear ($R_L = 1$), favorable ($0 < R_L < 1$), or irreversible ($R_L = 0$). The value for CFs was $R_L < 1$, indicating that the adsorption of Cr(VI) was favorable on this material.

3.6.2. Freundlich isotherm model

The Freundlich isotherm model relies on the assumption that the adsorption of metal ions takes place by multilayer adsorption on a heterogeneous surface, with interaction between the adsorbed molecules. This isotherm comes from an empirical equation that explains the exponential distribution of adsorption center of an adsorbent.[61] The linear form of Freundlich model using logarithms is represented by the following equation:

$$\log q_e = \log K_f + \frac{1}{n} \log C_e \qquad [6]$$

where q_e is the amount of Cr(VI) adsorbed per amount of adsorbent (mg/g), K_f (mg/g)(mg/L)^n and n are the Freundlich adsorption isotherm constants, and C_e is the equilibrium concentration of Cr(VI) in the solution (mg/L). A linear plot can be obtained between log q_e and log C_e, and then the values of K_F and $1/n$ are obtained from the intercept and slope by Equation (6).

Table 3. Isotherm model parameters for adsorption of Cr(VI) on CFs at different temperatures.

	Langmuir isotherm				Freundlich isotherm		
Temperatures (°C)	q_m (mg/g)	K_L	R_L	R^2	K_f (mg/g) (mg/L)^n	n	R^2
30	11.49	0.022	0.645	0.977	3.78	1.05	0.973
40	200.0	0.001	0.975	0.993	4.33	1.00	0.990
50	333.33	0.0008	0.979	0.974	1.08	1.13	0.951

The value of n (g/L) is an indication of the adsorption deviation from linearity and the value of $1/n$ is the heterogeneity factor. A value of n between 1 and 10 (i.e., $1/n < 1$) shows a favorable adsorption. For $n = 1$, linear adsorption is found; but for $n < 1$, adsorption becomes a chemical process; while for $n > 1$, adsorption is a physical process. In this study, $n > 1$ was found, showing that the adsorption of Cr(VI) ions onto CFs is a physical process.[62] If $1/n < 1$ a normal Langmuir isotherm is found, while for $1/n > 1$ a cooperative adsorption takes place.[63]

The results of the adsorption isotherms parameters are presented in Table 3. The results clearly show that the adsorption equilibrium value fits well with the Langmuir model as the R^2 values were much higher than those found for the Freundlich model. The CFs showed the maximum adsorption capacity (q_m) for the Cr(VI) ions to be 333.33 mg/g at 50 °C.

3.7. Adsorption kinetics

Four kinetic models (pseudo-first-order, pseudo-second-order, intra-particle diffusion l, and Elovich) were used to characterize the kinetics of adsorption of Cr(VI) on CFs. The study of the adsorption kinetics describes the rate of the adsorbate uptake on the adsorbent at different time intervals. The adsorption mechanism depends on the physical and chemical properties of the adsorbent. The mechanism of the rate control of the adsorption process depends on the diffusion, chemical reaction, and mass transfer.

3.7.1. Pseudo-first-order model

Lagergren's kinetic equation or pseudo-first-order equation[64] is most often used to describe the adsorption process of a substance present in the liquid phase. The linear form of the equation is:

$$\log(q_e - q_t) = \log q_e - \frac{K_1}{2.303} t \qquad [7]$$

where q_e and q_t (mg/g) are the quantity of Cr adsorbed at equilibrium and at a given time t, respectively, and k_1 is the pseudo-first-order rate constant. The linear plot of the pseudo-first-order model for adsorption of Cr(VI) ions on CFs is shown in Figure 7a. The plot of log (q_e – q_t) versus

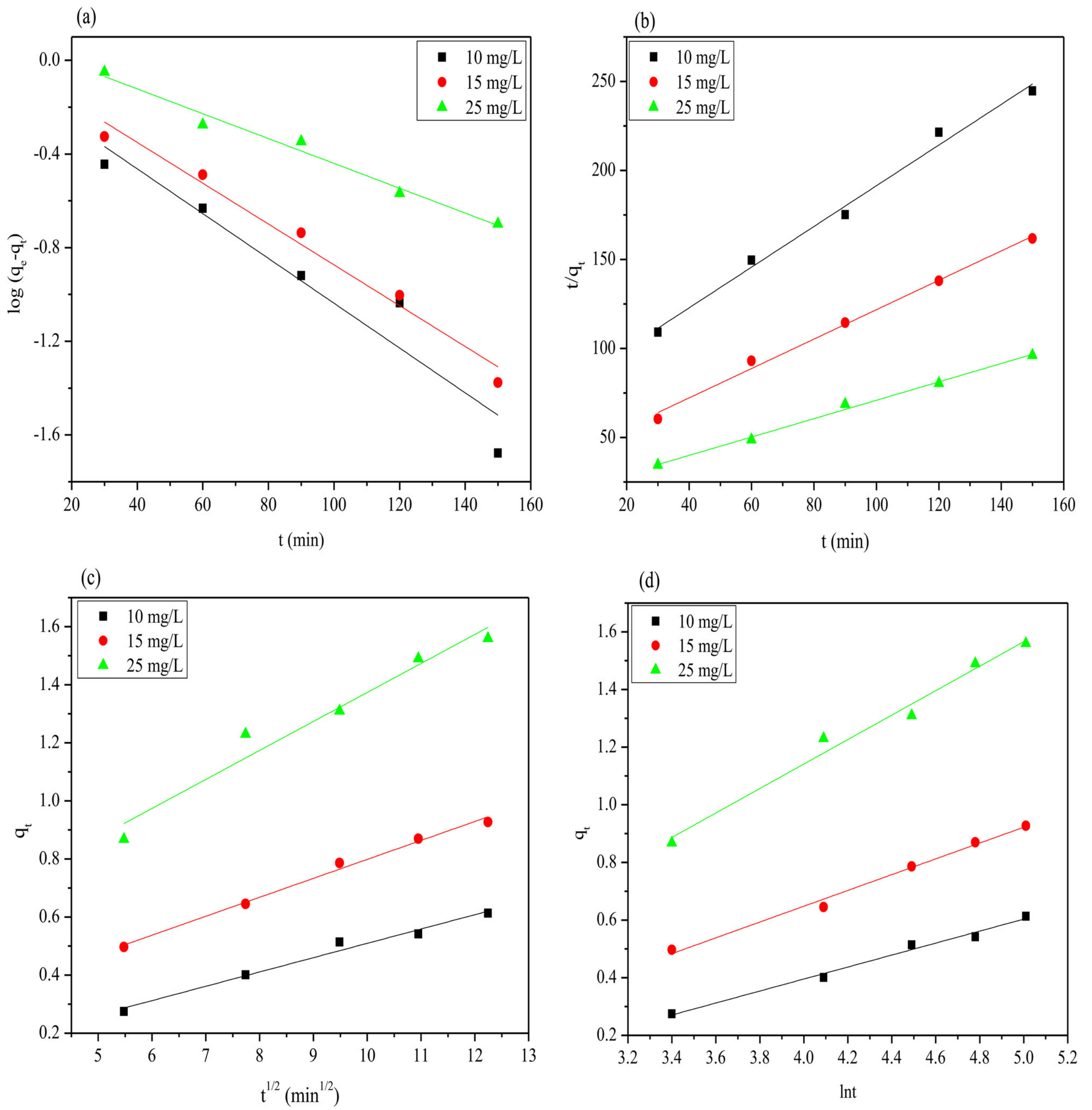

Figure 7. Adsorption kinetics. (a) Pseudo-first-order, (b) pseudo-second-order, (c) intra-particle diffusion , and (d) Elovich model plots of adsorption of Cr(VI) ions onto CFs at different initial concentration.

t was used to determine the pseudo-first-order rate constants k_1 and q_e and the coefficient of determination value (R^2).

Pseudo-first-order model had a poorer fit to the equilibrium data, owing to its boundary layer resistance.[65] From the results, the calculated q_e values did not match with the experimental values of q_e and the correlation coefficient (R^2) values seem to be comparatively very low than the other kinetic models.

3.7.2. Pseudo-second-order model

Ho and McKay[66] established the pseudo-second-order kinetic equation as:

$$\frac{t}{q_t} = \frac{1}{K_2 q_e^2} + \frac{t}{q_e} \tag{8}$$

where k_2 is the pseudo-second-order rate constant (g/mg/min). The linear plots of t/q_t versus t can be used to determine the pseudo-second-order rate constants k_2 and q_e from the slope and intercept, respectively. The results are shown in Figure 7b. Kinetic rate constant values decreased with the increase in the concentration of Cr(VI) onto CFs, which are shown in Table 4. This behavior is shown due to the decrease of surface site of the adsorbent with the increase of Cr(VI) ion concentration.[65] The calculated q_e values were more similar to the experimental values of q_e and the

Table 4. Parameters for different kinetic models fitted to the Cr(VI) adsorption kinetics on CFs at room temperature.

	C_0 (mg/L)		
Kinetic models and parameters	10	15	25
Pseudo-first-order			
q_e (exp.) (mg/g)	0.634	0.969	1.769
k_1 (min$-^{1}$)	0.020	0.018	0.011
q_e (cal.) (mg/g)	1.202	1.002	1.230
R^2	0.921	0.979	0.981
Pseudo-second-order			
k_2 (g mg^{-1} min^{-1})	0.017	0.017	0.014
q_e (cal.) (mg/g)	0.874	1.210	1.937
R^2	0.990	0.994	0.995
Elovich			
α (mg g^{-1})	0.436	0.448	0.556
β (mg g^{-1})	0.207	0.274	0.424
R^2	0.989	0.991	0.983
Intra-particle diffusion			
k_{id} (mg g^{-1} min$^{1/2}$)	0.049	0.065	0.099
C (mg g^{-1})	0.016	0.145	0.374
R^2	0.981	0.992	0.960

correlation coefficient (R^2) values were comparatively higher ($R^2 > 0.99$) than the other kinetic models.[67] Hence, pseudo-second-order kinetic model gave the best fit for Cr(VI) adsorption by CFs, which can be a rate-controlling step.

3.7.3. Intra-particle diffusion model

Weber and Morris[68] developed the intra-particle diffusion model which can be presented as:

$$q_t = K_{id} t^{1/2} + C \qquad [9]$$

where q_t (mg/g) is the amount of chromium(VI) adsorbed at time t (minutes) per unit of weight of CFs, k_{id} is the intra-particle diffusion rate constant (mg/g min$^{1/2}$), and C is the intercept. The linear plot of q_t versus $t^{1/2}$ is used to test a diffusion-controlled reaction. The increasing values of C indicate that there is an increase in boundary layer thickness of molecule which plays a major role of the surface adsorption in the rate-limiting step.[69] In Figure 7c, the linear fitting plot does not pass through the origin, which shows that the intra-particle diffusion is involved in the adsorption process but it is not the rate governing step for adsorption of Cr(VI) ions onto CFs.

3.7.4. Elovich model

Zeldowitsch describes the another kinetic equation for chemisorptions. The linear form of the Elovich equation is expressed as follows:

$$q_t = \frac{1}{\beta}\ln(\alpha\beta) + \frac{1}{\beta}\ln t \qquad [10]$$

where α is the Elovich initial adsorption rate constant (mg g^{-1}min^{-1}) and β is the desorption constant (g mg^{-1}). The Elovich parameters α and β can be calculated from the slope and intercept of the linear plot of q_t versus ln$t$, respectively (Figure 7d). The Elovich kinetic model explained the adsorption process better than the pseudo-first-order model. In addition, the results of Elovich model were in good agreement with pseudo-second-order kinetic model, which confirms the chemisorption nature of adsorption.[70] The values of parameters of Elovich model for Cr(VI) ions are given in Table 4.

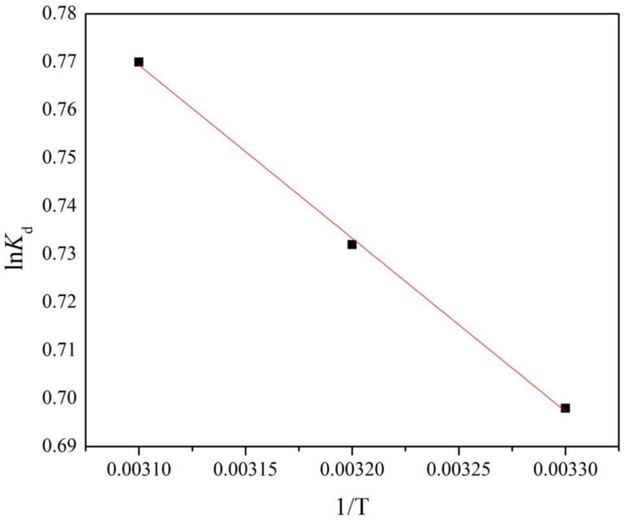

Figure 8. Van't Hoff's plot used to determine thermodynamic parameters for the removal of Cr(VI) by CFs.

The correlation coefficient (R^2) for Cr(VI) ions and the kinetic parameters are presented in Table 4. These data clearly show that the coefficients for the pseudo-second-order are closer to 1 and are higher for other kinetic models. Thus, the adsorption of Cr(VI) ions on CFs agrees with pseudo-second-order kinetics ($R^2 = 0.995$). These results show that chemisorption is the rate-controlling mechanism.

3.8. Adsorption thermodynamics

The thermodynamic parameters were determined using van't Hoff equation. The chromium adsorption on CFs was observed at three different temperatures at 30, 40, and 50 °C (303, 313, and 323 K) in optimized conditions. The change in Gibbs free energy (ΔG^0), change in entropy (ΔS^0), and change in enthalpy (ΔH^0), for the adsorption process were determined by the following equations.[71]

$$K_d = \frac{C_A}{C_B} \qquad [11]$$

$$\Delta G^0 = -RT\ln K_d \qquad [12]$$

$$\ln K_d = \frac{\Delta S^0}{R} - \frac{\Delta H^0}{RT} \qquad [13]$$

where K_d is the thermodynamic equilibrium constant, C_A is the equilibrium concentration of Cr(VI) ion adsorbed per litre on the CFs (mg/L), and C_B is the equilibrium Cr(VI) ion concentration (mg/L). R is the universal gas constant (8.314×10^{-3} kJ/mol K) and T is the absolute temperature in Kelvin (K). The values of ΔS^0 and ΔH^0 can be obtained from the slope and intercept of lnK_d versus $1/T$ van't Hoff plot, found in Figure 8.

The ΔH^0 and ΔS^0 values found were 2.99 kJ mol^{-1} and 15.42 J mol^{-1} K^{-1}, respectively. The positive value of enthalpy indicated that Cr(VI) adsorption was endothermic and the positive value of ΔS^0 confirmed the randomness of the solid–liquid interface during adsorption. The values of ΔG^0 were -1.75, -1.90, and -2.06 kJ mol^{-1} for 30, 40, and 50 °C, respectively, showing that the adsorption of Cr(VI) on CFs was thermodynamically favorable at all temperatures. The thermodynamic parameters are depicted in Table 5.

Table 5. Thermodynamic parameters for Cr(VI) adsorption on CFs.

			ΔG^0 (kJ/mol)		
C_0 (mg/L)	ΔH^0 (kJ/mol)	ΔS^0 (J/mol/K)	303 K	313 K	323 K
25.0	2.99	15.42	−1.75	−1.90	−2.06

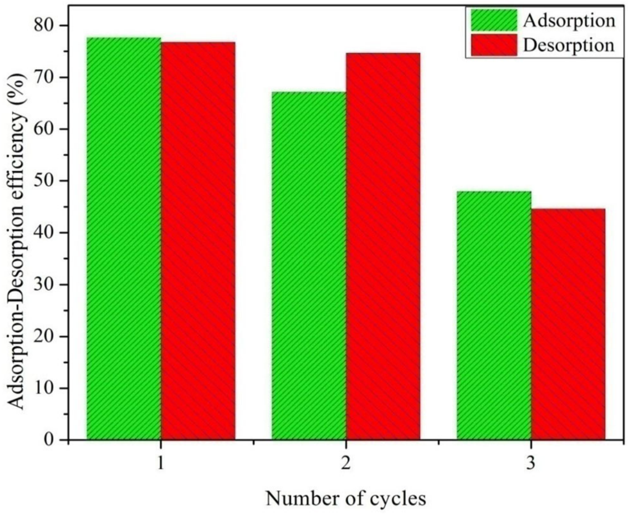

Figure 9. Adsorption–desorption cycles for CFs.

3.9. Desorption studies

Adsorbents can be re-used after a desorption process. Batch experiments were used for desorption studies. The regenerated CFs were re-used for the adsorption of Cr(VI) using the same initial concentration as for fresh CFs. Desorption studies were carried out for the Cr(VI) loaded CFs using a NaOH (0.5 M) solution as desorbing agent. CFs were re-used for three adsorption–desorption cycles and results are shown in Figure 9. 76.8% of the adsorbed Cr(VI) was desorbed from CFs using 0.5 M NaOH. Desorption is also a highly pH-dependent process. In acidic or neutral pH conditions, the weakly bonded adsorbate ions were removed partially but in alkaline solution (NaOH) they were completely desorbed due to the formation of soluble sodium chromate.[72] Higher concentrations of NaOH are useful for a more effective desorption and the successful regeneration of the adsorbents.

4. Adsorption mechanism

The mechanism of adsorption is very important to reveal the binding nature and properties of materials. As stated above, CFs consist of biopolymers with protonated amino, hydroxyl, and carboxylic groups, which provide active binding sites for metal ions. CFs have large surface areas with positive charge. Cr(VI) exists in five main stable forms in aqueous solution, namely H_2CrO_4, $HCrO_{4-}$, CrO_4^{2-}, $HCr_2O_7^{-}$, and $Cr_2O_7^{2-}$.

When CFs are placed into aqueous potassium dichromate solution, the negatively charged dichromate binds with the positively charged functional groups of the CFs, resulting in electrostatic attraction.

Affinity toward electronegative groups of keratin containing N, O, S varies with the properties of the metals which bind to

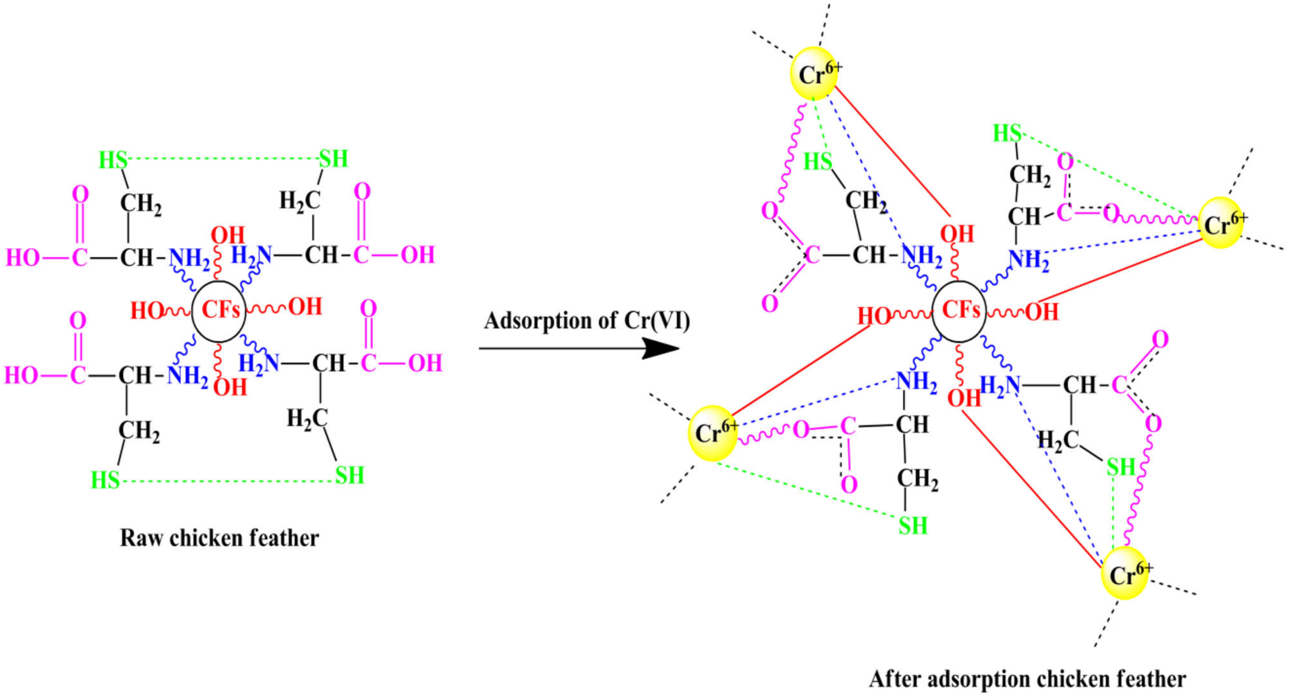

Figure 10. Mechanism of adsorption of Cr(VI) on CFs.

Table 6. Comparison of the maximum adsorption capacity of Cr(VI) by various waste materials used as adsorbents.

S. No.	Adsorbent materials	Adsorption capacity (mg/g)	pH	References
1.	Wheat bran	4.53	2.0	[75]
2.	Modified wheat bran	5.28	2.2	[75]
3.	Walnut shell	8.01	3.5	[76]
4.	Hazelnut shell	8.28	3.5	[76]
5.	Almond shell	3.40	3.2	[76]
6.	Coconut tree sawdust	3.46	3.0	[77]
7.	Sugarcane bagasse	1.76	2.0	[78]
8.	Rice husk	8.5	2.0	[79]
9.	Raw chicken feathers	333.33	2.5	Present work

the functional groups of NH_2, OH, SH, COOH. Metal cations are considered hard, soft, or intermediate Lewis acids and bind to soft or hard or intermediate bases. Metal centers are held by organic ligands present in the protein entity that is linked to electron donors of O, N, and S moieties, present in the protein or keratin, based on their electronegativities.[73]

The excellent mechanical properties are due to cross-linking; the source for the high strength of keratin with S-S and H-bonds, when dissolved in a suitable solvent, breaks and weakens. A similar amino acid sequence is noticed in feathered and clawed keratin species.[74] The chelate complex may result from the adsorption of metal ions that were active at hydroxyl, carboxyl, amino, thiol, and aromatic sites, in all groups being involved in the binding with metal (Cr) ions.

We can conclude that the electrostatic attraction and the ion exchange may be responsible for Cr(VI) adsorption on CFs. The probable mechanism is represented in Figure 10.

5. Comparison with other adsorbents

Table 6 shows the Cr(VI) adsorption capacity for CFs determined in this work, compared with other adsorbents reported in the literature. For the different adsorbents, the adsorption capacity varies according to the surface area. CFs have the added advantage of being low cost and readily available for the adsorption of Cr(VI) ions from the aqueous solution.

6. Conclusions

This study clearly shows that CFs are effective adsorbents for the removal of Cr(VI) ions from aqueous solution. Adsorption of Cr(VI) is a highly pH-dependent process and the optimum initial pH was 2.5. The maximum monolayer capacity (q_{max}) of CFs was found 333.33 mg/g at 50 °C in 180 minutes. Langmuir and Freundlich models were fitted at different temperatures and the experimental data were well described by the Langmuir adsorption model. The kinetics of Cr(VI) ions was explained by using pseudo-first-order, pseudo-second-order, intra-particle diffusion, and Elovich kinetic models, but pseudo-second-order showed the best fitting. The thermodynamics results showed that the process was endothermic and spontaneous. The reason of the adsorption of Cr(VI) ions is electrostatic attraction between Cr(VI) ion and CFs. CFs were re-usable in at least in three multiple cycles. Therefore, rachis of CFs may be a new kind of low-cost material which could convert Cr(VI) ions to the less toxic and more stable Cr(III) ions and could be used economically for the treatment of Cr(VI) contaminated wastewater.

List of symbols

C_0	initial concentrations of chromium (mg/L);
C_e	equilibrium concentration of chromium (mg/L);
V	volume of the solution (L);
m	amount of the adsorbent (g);
C_{des}	concentration of chromium after desorption (mg/L);
q_{max}	maximum adsorption capacity (mg/g);
q_e	amount of total chromium adsorbed per specific amount of adsorbent (mg/g);
K_L	Langmuir adsorption constant (L/mg);
R_L	separation factor (dimensionless);
R^2	correlation coefficient;
K_f	Freundlich isotherm constant (mg/g);
n	Freundlich constant (mg/g) $(\text{mg/L})^{1/n}$;
q_t	chromium ion adsorbed on adsorbent at a given time t (mg/g);
k_1	pseudo-first-order rate constant (min^{-1});
k_2	pseudo-second-order rate constant (g/mg min^{-1});
k_{id}	intra-particle diffusion rate constant (mg/g $\text{min}^{1/2}$);
C	intercept of intra-particle diffusion model;
α	Elovich initial adsorption rate constant (mg g^{-1} min^{-1});
β	desorption constant (g mg^{-1});
ΔG^0	Gibbs free energy change (kJ/mol);
ΔH^0	enthalpy (kJ/mol);
ΔS^0	entropy (J/mol/K);
R	universal gas constant (kJ/mol/K);
K_d	thermodynamic equilibrium constant;
T	temperature (K);

Acknowledgment

The authors are thankful to SAIF Centre STIC Kochi (Kerala) and NIT Raipur (Chhattisgarh) for providing instrumental facilities. The authors are also thankful to lab staff and research scholars at Department of Chemistry, Govt. V.Y.T. PG. Autonomous College, Durg (Chhattisgarh), India for their support.

Conflict of interest

There are no conflicts to declare.

Funding

This work has been supported by Fundação para a Ciência e a Tecnologia, Portugal (2020–2023 multiannual funding to Centro de Química Estrutural and Project UIDB/00100/2020). This work was also partially supported by the Associate Laboratory for Green Chemistry (LAQV), financed by national funds from FCT/MCTES (UIDB/50006/2020 and CEECINST/00102/2018) (Portugal).

ORCID

Ajaya Kumar Singh http://orcid.org/0000-0001-8180-7292
Sónia A. C. Carabineiro http://orcid.org/0000-0001-9913-4671

References

[1] Waseem, A.; Arshad, J.; Iqbal, F.; Sajjad, A.; Mehmood, Z.; Murtaza, G. Pollution Status of Pakistan: A Retrospective Review on Heavy Metal Contamination of Water, Soil, and Vegetables. *Biomed Res. Int.* **2014**, *2014*, 813206–813229. DOI: 10.1155/2014/813206.

[2] Chakarvorty, M.; Dwivedi, A. K.; Shukla, A. D.; Kumar, S.; Niyogi, A.; Usmani, M.; Pati, J. K. Geochemistry and Magnetic Measurements of Suspended Sediment in Urban Sewage Water Vis-a-Vis Quantification of Heavy Metal Pollution in Ganga and Yamuna Rivers, India. *Environ. Monit. Assess.* **2015**, *187*, 1–17. DOI: 10.1007/s10661-015-4794-x.

[3] Kumar, S.; Patra, C.; Narayanasamy, S.; Rajaraman, P. V. Performance of Acid-Activated Water Caltrop (*Trapa natans*) Shell in Fixed Bed Column for Hexavalent Chromium Removal from Simulated Wastewater. *Environ. Sci. Pollut. Res.* **2020**, *27*, 28042–28052. DOI: 10.1007/s11356-020-09155-8.

[4] Rangabhashiyam, S.; Giri Nandagopal, M. S.; Nakkeeran, E.; Selvaraju, N. Adsorption of Hexavalent Chromium from Synthetic and Electroplating Effluent on Chemically Modified *Swietenia mahagoni* Shell in a Packed Bed Column. *Environ. Monit. Assess.* **2016**, *188*, 1–13. DOI: 10.1007/s10661-016-5415-z.

[5] Rangabhashiyam, S.; Nakkeeran, E.; Anu, N.; Selvaraju, N. Biosorption Potentials of a Novel *Ficus auriculata* Leaves Powder for the Sequestration of Hexavalent Chromium from Aqueous Solutions. *Res. Chem. Intermed.* **2015**, *41*, 8405–8424. DOI: 10.1007/s11164-014-1900-6.

[6] Patra, C.; Medisetti, R. M. N.; Pakshirajan, K.; Narayanasamy, S. Assessment of Raw, Acid-Modified and Chelated Biomass for Sequestration of Hexavalent Chromium from Aqueous Solution Using *Sterculia villosa* Roxb. Shells. *Environ. Sci. Pollut. Res. Int.* **2019**, *26*, 23625–23637. DOI: 10.1007/s11356-019-05582-4.

[7] Nameni, M.; Alavi Moghadam, M. R.; Arami, M. Adsorption of Hexavalent Chromium from Aqueous Solutions by Wheat Bran. *Int. J. Environ. Sci. Technol.* **2008**, *5*, 161–168. DOI: 10.1007/BF03326009.

[8] Uysal, M.; Irfan, A. Removal of Cr(VI) from Industrial Wastewaters by Adsorption Part I: Determination of Optimum conditions. *J. Hazard. Mater.* **2007**, *149*, 482–491. DOI: 10.1016/j.jhazmat.2007.04.019.

[9] Rengaraj, S.; Joo, C. K.; Kim, Y.; Yi, J. Kinetics of Removal of Chromium from Water and Electronic Process Wastewater by Ion Exchange Resins: 1200H, 1500H and IRN97H. *J. Hazard. Mater.* **2003**, *102*, 257–275. DOI: 10.1016/S0304-3894(03)00209-7.

[10] Kozlowski, C. A.; Walkowiak, W. Removal of Chromium(VI) from Aqueous Solutions by Polymer Inclusion Membranes. *Water Res.* **2002**, *36*, 4870–4876. DOI: 10.1016/s0043-1354(02)00216-6.

[11] Li, C.; Chen, H.; Li, Z. Adsorptive Removal of Cr(VI) by Fe-Modified Steam Exploded Wheat Straw. *Proc. Biochem.* **2004**, *39*, 541–545. DOI: 10.1016/s0032-9592(03)00087-6.

[12] Yu, R.; Yu, X.; Xue, B.; Liao, J.; Zhu, W.; Tian, S. Adsorption of Chlortetracycline from Aquaculture Wastewater Using Modified Zeolites. *J. Environ. Sci. Health Part A* **2020**, *55*, 573–584. DOI: 10.1080/10934529.2020.1717275.

[13] Patra, C.; Shahnaz, T.; Subbiah, S.; Narayanasamy, S. Comparative Assessment of Raw and Acid-Activated Preparations of Novel *Pongamia pinnata* Shells for Adsorption of Hexavalent Chromium from Simulated Wastewater. *Environ. Sci. Pollut. Res. Int.* **2020**, *27*, 14836–14851. DOI: 10.1007/s11356-020-07979-y.

[14] Chakraborty, R.; Asthana, A.; Singh, A. K.; Jain, B.; Susan, M. A. B. H. Adsorption of Heavy Metal Ions by Various Low Cost Adsorbents: A Review. *Int. J. Environ. Anal. Chem.* **2020**. DOI: 10.1080/03067319.2020.1722811.

[15] Gupta, V. K.; Nayak, A.; Agarwal, S. Bioadsorbents for Remediation of Heavy Metals: Current Status and Their Future Prospects. *Environ. Eng. Res.* **2015**, *20*, 1–18. DOI: 10.4491/eer.2015.018.

[16] Huang, K.; Xiu, Y.; Zhu, H. Selective Removal of Cr(VI) from Aqueous Solution by Adsorption on Mangosteen Peel. *Environ. Sci. Pollut. Res. Int.* **2013**, *20*, 5930–5938. DOI: 10.1007/s11356-013-1497-0.

[17] Ullah, I.; Nadeem, R.; Iqbal, M.; Manzoor, Q. Biosorption of Chromium onto Native and Immobilized Sugarcane Bagasse Waste Biomass. *Ecol. Eng.* **2013**, *60*, 99–107. DOI: 10.1016/j.ecoleng.2013.07.028.

[18] Chakraborty, R.; Verma, R.; Asthana, A.; Sree Vidya, S.; Singh, A. K. Adsorption of Hazardous Chromium (VI) Ions from Aqueous Solutions Using Modified Sawdust: Kinetics, Isotherm and Thermodynamic Modelling. *Int. J. Environ. Anal. Chem.* **2019**. DOI: 10.1080/03067319.2019.1673743.

[19] Yi, Y.; Lv, J.; Liu, Y.; Wu, G. Synthesis and Application of Modified Litchi Peel for Removal of Hexavalent Chromium from Aqueous Solutions. *J. Mol. Liq.* **2017**, *225*, 28–33. DOI: 10.1016/j.molliq.2016.10.140.

[20] Sostaric, T. D.; Petrovic, M. S.; Pastor, F. T.; Loncarevic, D. R.; Petrovic, J. T.; Milojkovic, J. V.; Stojanovic, M. D. Study of Heavy Metals Biosorption on Native and Alkali-Treated Apricot Shells and Its Application in Wastewater Treatment. *J. Mol. Liq.* **2018**, *259*, 340–349. DOI: 10.1016/j.molliq.2018.03.055.

[21] Yunus, Z. M.; Othman, N.; Al-Gheethi, A.; Hamdan, R.; Ruslan, N. N. Adsorption of Heavy Metals from Mining Effluents Using Honeydew Peels Activated Carbon; Isotherm, Kinetic and Column Studies. *J. Dispers. Sci. Technol.* **2019**. DOI: 10.1080/01932691.2019.1709493.

[22] Reddy, N.; Yang, Y. Structure and Properties of Chicken Feather Barbs as Natural Protein Fibers. *J. Polym. Environ.* **2007**, *15*, 81–87. DOI: 10.1007/s10924-007-0054-7.

[23] Barone, J. R.; Schmidt, W. F. Effect of Formic Acid Exposure on Keratin Fiber Derived from Poultry Feather Biomass. *Bioresour. Technol.* **2006**, *97*, 233–242. DOI: 10.1016/j.biortech.2005.02.039.

[24] Banat, F.; Al-Asheh, S.; Al-Rousan, D. Comparison between Different Keratin Composed Biosorbents for the Removal of Heavy Metal Ions from Aqueous Solutions. *Adsorpt. Sci. Technol.* **2002**, *20*, 393–416. DOI: 10.1260/02636170260295579.

[25] Al-Asheh, S.; Banat, F.; Al-Rousan, D. Adsorption of Copper, Zinc and Nickel Ions from Single and Binary Metal Ion Mixtures on to Chicken Feathers. *Adsorpt. Sci. Technol.* **2002**, *20*, 849–864. DOI: 10.1260/02636170260555778.

[26] de la Rosa, G.; Reynel-Avila, H. E.; Bonilla-Petriciolet, A.; Cano-Rodríguez, I.; Velasco-Santos, C.; Martinez-Hernandez, A. L. Recycling Poultry Feathers for Pb Removal from Wastewater: Kinetic and Equilibrium Studies. *Int. J. Chem. Biomol. Eng.* **2008**, *1*, 185–193. DOI: 10.5281/zenodo.1062126.

[27] Mittal, A.; Kurup, L.; Mittal, J. Freundlich and Langmuir Adsorption Isotherms and Kinetics for the Removal of Tartrazine from Aqueous Solutions Using Hen Feathers. *J. Hazard. Mater.* **2007**, *146*, 243–248. DOI: 10.1016/j.jhazmat.2006.12.012.

[28] Mittal, A. Use of Hen Feathers as Potential Adsorbent for the Removal of a Hazardous Dye, Brilliant Blue FCF, from Wastewater. *J. Hazard. Mater.* **2006**, *128*, 233–239. DOI: 10.1016/j.jhazmat.2005.08.043.

[29] Mittal, A. Adsorption Kinetics of Removal of a Toxic Dye, Malachite Green, from Wastewater by Using Hen Feathers. *J. Hazard. Mater.* **2006**, *133*, 196–202. https://doi.org/j.jhazmat.2005.10.017. DOI: 10.1016/j.jhazmat.2005.10.017.

[30] Gupta, V. K.; Mittal, A.; Kurup, L.; Mittal, J. Adsorption of a Hazardous Dye, Erythrosine, over Hen Feathers. *J. Colloid Interface Sci.* **2006**, *304*, 52–57. DOI: 10.1016/j.jcis.2006.08.032.

[31] Reynel-Avila, H. E.; de la Rosa, G.; Rojas-Mayorga, C. K.; Cano-Aguilera, I.; Bonilla-Petriciolet, A. Kinetic and Thermodynamic Modeling of Cd^{2+} and Ni^{2+} Biosorption of Raw Chicken Feathers. *Int. J. Chem. Reactor Eng.* **2011**, *9*, 1–26. DOI: 10.2202/1542-6580.2752.

[32] Aguayo-Villarreal, I. A.; Bonilla-Petriciolet, A.; Hernandez-Montoya, V.; Montes-Moran, M. A.; Reynel-Avila, H. E. Batch

and Column Studies of Zn^{2+} Removal from Aqueous Solution Using Chicken Feathers as Sorbents. *Chem. Eng. J.* **2011**, *167*, 67–76. DOI: 10.1016/j.cej.2010.11.107.

[33] Al-Asheh, S.; Banat, F.; Al-Rousan, D. Beneficial Reuse of Chicken Feathers in Removal of Heavy Metals from Waste Water. *J. Clean. Prod.* **2003**, *11*, 321–326. DOI: 10.1016/S0959-6526(02)00045-8.

[34] Chakraborty, R.; Asthana, A.; Singh, A. K.; Yadav, S.; Susan, M. A. B. H.; Carabineiro, S. A. C. Intensified Elimination of Aqueous Heavy Metal Ions Using Chicken Feathers Chemically Modified by a Batch Method. *J. Mol. Liq.* **2020**, *312*, 113475. DOI: 10.1016/j.molliq.2020.113475.

[35] Garg, V. K.; Gupta, R.; Kumar, R.; Gupta, R. K. Adsorption of Chromium from Aqueous Solution on Treated Sawdust. *Bioresour. Technol.* **2004**, *92*, 79–81. DOI: 10.1016/j.biortech.2003.07.004.

[36] Kołodyńska, D.; Krukowska, J.; Thomas, P. Comparison of Sorption and Desorption Studies of Heavy Metal Ions from Biochar and Commercial Active Carbon. *Chem. Eng. J.* **2017**, *307*, 353–363. DOI: 10.1016/j.cej.2016.08.088.

[37] Gao, P.; Liu, Z.; Wu, X.; Cao, Z.; Zhuang, Y.; Sun, W.; Xue, G.; Zhou, M. Biosorption of Chromium (VI) Ions by Deposits Produced from Chicken Feathers after Soluble Keratin Extraction. *CLEAN Soil Air Water* **2014**, *42*, 1558–1566. DOI: 10.1002/clen.201300669.

[38] Vasconcelos, A.; Freddi, G.; Cavaco-Paulo, A. Biodegradable Materials Based on Silk Fibroin and Keratin. *Biomacromolecules* **2008**, *9*, 1299–1305. DOI: 10.1021/bm9002927.

[39] Iqbal, M.; Saeed, A.; Zafar, S. I. FTIR Spectroscopy, Kinetics and Adsorption Isotherm Modeling, Ion Exchange and EXD Analysis of Understanding the Mechanism of Cd^{2+} and Pb^{2+} Removal by Mango Peel Waste. *J. Hazard. Mater.* **2009**, *164*, 161–171. DOI: 10.1016/j.jhazmat.2008.07.141.

[40] Rao, R. A. K.; Rehman, F. Adsorption Studies on Fruits of Gular (*Ficus glomerata*): Removal of Cr(VI) from Synthetic Wastewater. *J. Hazard. Mater.* **2010**, *181*, 405–412. DOI: 10.1016/j.jhazmat.2010.05.025.

[41] Kar, P.; Misra, M. Use of Keratin Fiber for Separation of Heavy Metals from Water. *J. Chem. Technol. Biotechnol.* **2004**, *79*, 1313–1319. DOI: 10.1002/jctb.1132.

[42] Aravind, J.; Sudha, G.; Kanmani, P.; Devisri, A. J.; Dhivyalakshmi, S.; Raghavprasad, M. Equilibrium and Kinetic Study on Chromium (VI) Removal from Simulated Waste Water Using Gooseberry Seeds as a Novel Biosorbent. *Global J. Environ. Sci. Manage.* **2015**, *1*, 233–244. DOI: 10.7508/GJESM.2015.03.006.

[43] Hong, X.; Fang, C.; Hui, K. S.; Hui, K. N.; Zhuang, H.; Liu, W.; Shan, S. Influence of Interfering Anions on Cu^{2+} and Zn^{2+} Ions Removal on Chestnut Outer Shell-Derived Hydrochars in Aqueous Solution. *RSC Adv.* **2017**, *7*, 51199–51205. DOI: 10.1039/C7RA10384K.

[44] Khalid, R.; Aslam, Z.; Abbas, A.; Ahmad, W.; Ramzan, N.; Shawabkeh, R. Adsorptive Potential of Acacia Nilotica Based Adsorbent for Chromium (VI) from an Aqueous Phase. *Chin. J. Chem. Eng.* **2018**, *26*, 614–622. DOI: 10.1016/j.cjche.2017.08.017.

[45] Khosa, M. A.; Ullah, A. In-Situ Modification, Regeneration, and Application of Keratin Biopolymer for Arsenic Removal. *J. Hazard. Mater.* **2014**, *278*, 360–371. DOI: 10.1016/j.jhazmat.2014.06.023.

[46] El-Latif, M. M. A.; Ibrahim, A. M. Adsorption, Kinetic and Equilibrium Studies on Removal of Basic Dye from Aqueous Solutions Using Hydrolyzed Oak Sawdust. *Desalin. Water Treat.* **2009**, *6*, 252–268. DOI: 10.5004/dwt.2009.501.

[47] Kumar, R.; Sharma, R. K. Synthesis and Characterization of Cellulose Based Adsorbents for Removal of Ni(II), Cu(II) and Pb(II) Ions from Aqueous Solutions. *React. Funct. Polym.* **2019**, *140*, 82–92. DOI: 10.1016/j.reactfunctpolym.2019.04.014.

[48] Liang, S.; Ye, N.; Hu, Y.; Shi, Y.; Zhang, W.; Yu, W.; Wu, X.; Yang, J. Lead Adsorption from Aqueous Solutions by a Granular Adsorbent Prepared from Phoenix Tree Leaves. *RSC Adv.* **2016**, *6*, 25393–25400. DOI: 10.1039/C6RA03258C.

[49] Mondal, M. K. Removal of Pb(II) from Aqueous Solution by Adsorption Using Activated Tea Waste. *Korean J. Chem. Eng.* **2010**, *27*, 144–151. DOI: 10.1007/s11814-009-0304-6.

[50] Sun, X.; Li, Q.; Yang, L.; Liu, H. Chemically Modified Magnetic Chitosan Microspheres for Cr(VI) Removal from Acidic Aqueous Solution. *Particuology* **2016**, *26*, 79–86. DOI: 10.1016/j.partic.2015.11.003.

[51] Shang, T. X.; Zhang, J.; Jin, X. J.; Gao, J. M. Study of Cr(VI) Adsorption onto Nitrogen-Containing Activated Carbon Preparation from Bamboo Processing Residues. *J. Wood Sci.* **2014**, *60*, 215–224. DOI: 10.1007/s10086-014-1392-4.

[52] Georgieva, V. G.; Tavlieva, M. P.; Genieva, S. D.; Vlaev, L. T. Adsorption Kinetics of Cr(VI) Ions from Aqueous Solutions onto Black Rice Husk Ash. *J. Mol. Liq.* **2015**, *208*, 219–226. DOI: 10.1016/j.molliq.2015.04.047.

[53] Verma, A.; Chakraborty, S.; Basu, J. K. Adsorption Study of Hexavalent Chromium Using Tamarind Hull-Based Adsorbents. *Sep. Purif. Technol.* **2006**, *50*, 336–341. DOI: 10.1016/j.seppur.2005.12.007.

[54] Nemr, A. E. Potential of Pomegranate Husk Carbon for Cr(VI) Removal from Wastewater: Kinetic and Isotherm Studies. *J. Hazard. Mater.* **2009**, *161*, 132–141. DOI: 10.1016/j.jhazmat.2008.03.093.

[55] Singha, B.; Das, S. K. Biosorption of Cr(VI) Ions from Aqueous Solutions: Kinetics, Equilibrium, Thermodynamics and Desorption Studies. *Colloids Surf. B Biointerfaces* **2011**, *84*, 221–232. DOI: 10.1016/j.colsurfb.2011.01.004.

[56] Prabhakaran, S. K.; Vijayaraghavan, K.; Balasubramanian, R. Removal of Cr(VI) Ions by Spent Tea and Coffee Dusts Reduction to Cr(III) and Biosorption. *Ind. Eng. Chem. Res.* **2009**, *48*, 2113–2117. DOI: 10.1021/ie801380h.

[57] Gupta, V. K.; Rastogi, A. Biosorption of Hexavalent Chromium by Raw and Acid-Treated Green Alga *Oedogonium hatei* from Aqueous Solutions. *J. Hazard. Mater.* **2009**, *163*, 396–402. DOI: 10.1016/j.jhazmat.2008.06.104.

[58] Yu, L. J.; Shukla, S. S.; Dorris, K. L.; Shukla, A.; Margrave, J. L. Adsorption of Chromium from Aqueous Solutions by Maple Sawdust. *J. Hazard. Mater. B* **2003**, *100*, 53–63. DOI: 10.1016/s0304-3894(03)00008-6.

[59] Shahnaz, T.; Patra, C.; Sharma, V.; Selvaraju, N. A Comparative Study of Raw, Acid-Modified and EDTA-Complexed *Acacia auriculiformis* Biomass for the Removal of Hexavalent Chromium. *Chem. Ecol.* **2020**, *36*, 360–381. DOI: 10.1080/02757540.2020.1723560.

[60] Langmuir, I. The Constitution and Fundamental Properties of Solids and Liquids. *J. Am. Chem. Soc.* **1916**, *38*, 2221–2295. DOI: 10.1021/ja02268a002.

[61] Freundlich, H. M. F. Uber die adsorption in lasungen. *J. Phys. Chem.* **1906**, *57*, 385–470.

[62] Kumar, P. S.; Ramalingam, S.; Sathyaselvabala, V.; Kirupha, S. D.; Murugesan, A.; Sivanesan, S. Removal of Cadmium(II) from Aqueous Solution by Agricultural Waste Cashew Nut Shell. *Korean J. Chem. Eng.* **2012**, *29*, 756–768. DOI: 10.1007/s11814-011-0259-2.

[63] Fytianos, K.; Voudrias, E.; Kokkalis, E. Sorption-Desorption Behaviour of 2.4-Dichlorophenol by Marine Sediments. *Chemosphere* **2000**, *40*, 3–6. DOI: 10.1016/s0045-6535. (99)00214-3.

[64] Lagergren, S. About the Theory of So-Called Adsorption of Soluble Substances. *K. Sven. Vet. Akad. Handl.* **1898**, *24*, 1–39.

[65] Saranya, N.; Nakkeeran, E.; Shrihari, S.; Selvaraju, N. Equilibrium and Kinetic Studies of Hexavalent Chromium Removal Using a Novel Biosorbent: *Ruellia patula* Jacq. *Arab. J. Sci. Eng.* **2017**, *42*, 1545–1557. DOI: 10.1007/s13369-017-2416-3.

[66] Ho, Y. S.; McKay, G. Pseudo-Second Order Model for Sorption Processes. *Process Biochem.* **1999**, *34*, 451–465. DOI: 10.1016/s0032-9592(98)00112-5.

[67] Saranya, N.; Nakeeran, E.; Giri Nandagopal, M. S.; Selvaraju, N. Optimization of Adsorption Process Parameters by Response Surface Methodology for Hexavalent Chromium Removal from

Aqueous Solutions Using *Annona reticulata* Linn Peel Microparticles. *Water Sci Technol* **2017**, *75*, 2094–2107. DOI: 10.2166/wst.2017.092.

[68] Weber, W. J.; Morris, J. C. *Advances in Water Pollution Research: Removal of Biologically Resistant Pollutants from Waste Waters by Adsorption*. Presented at the Proceedings of International Conference on Water Pollution Symposium, Pergamon Press, Oxford, UK, **1962**, Vol. 2, pp. 231–266.

[69] Nakkeeran, E.; Saranya, N.; Giri Nandagopal, M. S.; Santhiagu, A.; Selvaraju, N. Hexavalent Chromium Removal from Aqueous Solutions by a Novel Powder Prepared from Colocasia esculenta Leaves. *Int. J. Phytoremediation* **2016**, *18*, 812–821. DOI: 10.1080/15226514.2016.1146229.

[70] Khan, T. A.; Chaudhry, S. A.; Ali, I. Thermodynamic and Kinetic Studies of As(V) removal from Water by Zirconium Oxide-Coated Marine Sand. *Environ. Sci. Pollut. Res. Int.* **2013**, *20*, 5425–5440. DOI: 10.1007/s11356-013-1543-y.

[71] Mohan, D.; Singh, K. P. Single- and Multi-Component Adsorption of Cadmium and Zinc Using Activated Carbon Derived from Bagasse: An Agricultural Waste. *Water Res.* **2002**, *36*, 2304–2318. DOI: 10.1016/s0043-1354(01)00447-X.

[72] Singh, K. K.; Rastogi, R.; Hasan, S. H. Removal of Cr(VI) from Wastewater Using Rice Bran. *J. Colloid Interface Sci.* **2005**, *290*, 61–68. DOI: 10.1016/j.jcis.2005.04.011.

[73] Whitford, D. *Proteins Structure and Function*; John Wiley & Sons Ltd: Chichester, **2005**.

[74] Placido Moore, G. R.; Martelli, S. M.; Gandolfo, C.; Amaral Sobral, P. J.; Laurindo, L. B. Influence of the Glycerol Concentration on Some Physical Properties of Feather Keratin Films. *Food Hydrocolloids* **2006**, *20*, 975–982. DOI: 10.1016/j.foodhyd.2005.11.001.

[75] Kaya, K.; Pehlivan, E.; Schmidt, C.; Bahadir, M. Use of Modified Wheat Bran for the Removal of Chromium(VI) from Aqueous Solutions. *Food Chem.* **2014**, *158*, 112–117. DOI: 10.1016/j.foodchem.2014.02.107.

[76] Pehlivan, E.; Altun, T. Biosorption of Chromium(VI) Ion from Aqueous Solutions Using Walnut, Hazelnut and Almond Shell. *J. Hazard. Mater.* **2008**, *155*, 378–384. DOI: 10.1016/j.jhazmat.2007.11.071.

[77] Selvi, K.; Pattabhi, S.; Kadirvelu, K. Removal of Cr(VI) from Aqueous Solution by Adsorption onto Activated Carbon. *Bioresour. Technol.* **2001**, *80*, 87–89. DOI: 10.1016/s0960-8524(01)00068-2.

[78] Aloma, I. C.; Rodriguez, I.; Calero, M.; Blazquez, G. Biosorption of Cr^{6+} from Aqueous Solution by Sugarcane Bagasse. *Desalin. Water Treat.* **2014**, *52*, 5912–5922. DOI: 10.1080/19443994.2013.812521.

[79] Bansal, M.; Garg, U.; Singh, D.; Garg, V. K. Removal of Cr(VI) from Aqueous Solutions Using Pre-Consumer Processing Agricultural Waste: A Case Study of Rice Husk. *J. Hazard. Mater.* **2009**, *162*, 312–320. DOI: 10.1016/j.jhazmat.2008.05.037.